



ELSEVIER

Journal of Chromatography A, 725 (1996) 351–359

JOURNAL OF
CHROMATOGRAPHY A

Continuous chromatomembrane headspace analysis

L.N. Moskvina*, O.V. Rodinkov

Department of Chemistry, St. Petersburg State University, 2 Universitetsky pr., Petrodvorets, St. Petersburg 198904, Russian Federation

First received 21 February 1995; revised manuscript received 1 September 1995; accepted 1 September 1995

Abstract

A novel version of headspace analysis is substantiated by theory and experiment. The version assumes chromatomembrane extraction of the analyte components into a gas phase. The boundary conditions for the process of chromatomembrane gas extraction are established. Two modes are suggested for analysis with continuous extraction of analyte substances: the mode of ultimate equilibrium saturation and that of total isolation. The advantages of the method in the determination of traces of volatile substances are obvious from its comparison with traditional techniques based on stripping or membrane diffusion.

Keywords: Headspace analysis; Chromatomembrane

1. Introduction

Two basic versions of headspace analysis (HSA) have found wide application in analytical practice. The first is a static method in which definite volumes of liquid sample and extracting gas are equilibrated in an isolated system. The second is a dynamic method in which the extracting gas flow is passed through the liquid sample volume immediately (stripping) or along the gas-permeable membrane in contact with the liquid [1–3]. The technical level of designs for realizing the gas extraction process determines the analytical possibilities of both methods. The surface area between the liquid and gas phases does not gain high values for stripping and or for the stationary version. As a result, the time for

inter-phase equilibrium to be established can take tens of minutes, which surpasses substantially the duration of the subsequent gas-chromatographic analysis [4,5]. This is the reason to continue to search for new instrumental concepts even though several companies have been producing HSA equipment for years. The main problems here arise in the continuous extraction of analyte substances from the flow of monitored medium (see Refs. [6] and [7], for instance). A chromatomembrane method for the separation of substances, based on capillary phenomena within hydrophobic porous media [8], opens up new prospects for HSA.

2. Theory

The chromatomembrane mass-exchange pro-

* Corresponding author.

cess is realized between a polar liquid phase and a non-polar liquid or gas phase within a hydrophobic biporous medium. The polar liquid should not wet the medium. The medium must preferentially have two types of open pores differing in size. To prevent capillary effects in macropores, their size should exceed the value derived from the known expression

$$P_C = \frac{2\sigma \cos \theta}{r} \quad (1)$$

where σ is the surface tension of the liquid phase, θ the contact angle between the liquid and the membrane material and r the pore radius. In the case of polytetrafluoroethylene (PTFE) porous matrix with a contact angle of 108° the capillary effects become negligible within pores of 0.1 mm radius. In turn, the size of the micropores should provide a capillary pressure that will prevent the penetration of polar liquid phase from the macropores into the micropores. Independent inlet and outlet of flows of the two phases is possible when the biporous medium is bounded by microporous membranes on two sides—those of the inlet and outlet of non-polar liquid or gas phase. The membranes should be made of the same material as the biporous matrix and have a pore size identical with that of micropores of the matrix. To provide mutual connections between the micropores of the biporous medium and those of membranes, the medium and the bounding membranes are made in the form of an integral three-layer unit (Fig. 1).

With these conditions, it is possible to organize within the same biporous matrix independent flows of two phases: polar liquid and gas or polar and non-polar liquid phases. The absence of flow mixing of liquid and gas phases that move within the macropores and micropores, respectively, in the case of gas extraction from polar liquids, is guaranteed when the conditions

$$P_{L1} < P_{G2} + |P_C| \quad (2)$$

and

$$P_{G1} < P_{L2} \quad (3)$$

are valid, where P_{L1} and P_{L2} are the liquid-phase

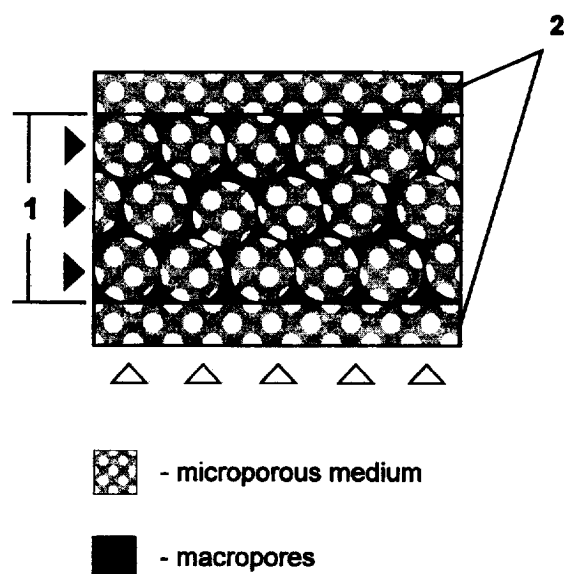


Fig. 1. Scheme of the chromatomembrane process. 1 = Mass-exchange layer; 2 = membranes. ▲ = Flow of the polar liquid; △ = flow of the non-polar liquid or gas.

pressures at the inlet and outlet of the mass-exchange space of the chromatomembrane cell, respectively, P_{G1} and P_{G2} are the gas-phase pressures at the inlet and outlet of the mass-exchange space, respectively, and P_C is the capillary pressure in the micropores. The flow-rates, with all other factors being fixed, will depend on pressure gradients within the mass-exchange space of the cell. Combining Eqs. 2 and 3, we obtain, after simple transformation, the following expression:

$$P_{L1} - P_{L2} + P_{G1} - P_{G2} = \Delta P_L + \Delta P_G < |P_C| \quad (4)$$

Hence it is necessary for the chromatomembrane process that the sum of pressure gradients for the liquid and gas phases should be less than the absolute capillary pressure value. The latter is the main physico-chemical parameter that defines the capabilities of the method.

Let us consider the principles for changes in the permeability of the chromatomembrane cell vs. the pore size in order to estimate limiting flow rates that may be achieved within the cell. For approximate calculation of the flux of a phase

through the cell we use the well known Hagen-Poiseuille equation:

$$W = \frac{\pi r^4 \Delta P}{8\eta l} \quad (5)$$

where W is the flux of a liquid or a gas through the capillary (m^3/s), r the capillary radius (m), P the pressure gradient (N/m^2), η the viscosity of the medium ($\text{N s}/\text{m}^2$), and l the capillary length (m). This equation is valid for a single capillary. We may consider as a rough assumption the mass-exchange layer to be a system of parallel micro- and macro-capillaries that are placed perpendicular to each other. When adopting this model, the rate of flow through the mass-exchange layer along each direction will depend on the number of unitary capillaries of each type and their permeability. The number of capillaries is calculated as the ratio of the volume fraction of the mass-exchange layer occupied with the given pore type to the volume of a theoretical single capillary of corresponding radius. With these assumptions, the equation for calculation of phase flux through the chromatomembrane cell can be written as

$$W = \frac{r^2 \Delta P S_c D}{8\eta l_c} \quad (6)$$

where S_c is the area of the chromatomembrane cell cross-section (perpendicular to the direction of the given phase flow), l_c the dimension of the cell along this direction and D the volume fraction of the cell occupied with the given phase.

Let us consider an ideal chromatomembrane cell with the mass-exchange layer dimension $1 \times 1 \times 1$ cm. The volume fractions of micro- and macropores within the cell are equal: 0.3. The assumed values are close to the experimentally obtained volume fractions of PTFE chromatomembrane cells filled with gas phase and aqueous solution. The pressure drop ΔP_L should be within the range 0.01–0.10 bar to create an aqueous phase flux through the cell within the range 10–100 cm^3/min . This follows from calculations according to Eq. 6 and it is confirmed with experimental data. The ΔP_L value can be

essentially greater only for highly viscous polar liquids.

The maximum allowable value for the pressure drop ΔP_G of the gas phase one can obtain from the Eq. 4 condition for realization of the chromatomembrane process is

$$\Delta P_G = |P_C| - \Delta P_L \quad (7)$$

The admissible gradient of gas-phase pressure rises, along with the absolute P_C value, with decrease in the pore radius according to Eq. 1. On the other hand, with the same pressure gradient, the flow-rate of the gas phase according to Eq. 6 will decrease sharply with decrease in the pore radius. The optimum may be chosen taking into account these two contrasting tendencies.

Fig. 2 shows plots for the maximum rates of gas (nitrogen) flow through the ideal chromatomembrane cell vs. the micropore radius. The data were calculated according to Eq. 6 for maximum admissible gas-phase pressure gradients obtained from Eq. 7. The rates are plotted for two values of ΔP_L : 0.03 and 0.1 bar. We

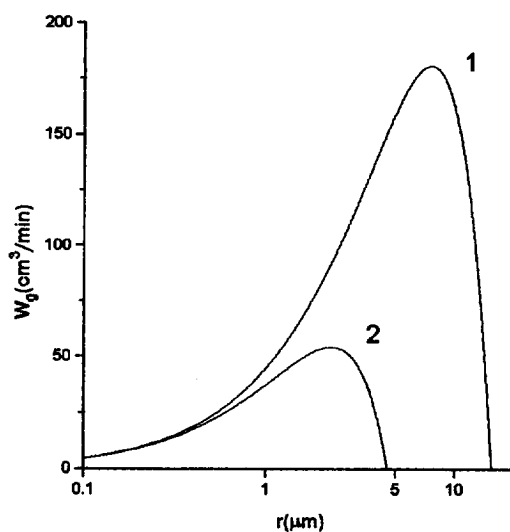


Fig. 2. Ultimate flux of nitrogen (W_G) through an ideal chromatomembrane cell calculated as a function of the radius of membrane micropores (r) with the pressure gradient of an aqueous phase (ΔP_w) being fixed. Cell dimensions $1 \times 1 \times 1$ cm with boundary membranes 1 mm thick. (1) $\Delta P_w = 0.03$ bar; (2) $\Delta P_w = 0.1$ bar.

assumed the contact angle to be 108° , which corresponds to PTFE as a material for the mass-exchange layer and the membranes.

The data indicate that the chromatomembrane process can be realized within a broad range of rates of liquid and gas phases. The maximum admissible flow-rates can be gained with micropores of $2\text{--}5\ \mu\text{m}$ radius, but it is necessary that all the micropores have similar sizes to obtain these flows. Ideally, to realize the chromatomembrane process one must obtain porous hydrophobic materials with no dispersion of pore sizes. Considering the common porous materials, the upper limit of the pore size distribution will be the criterion that will determine the maximum admissible flow-rates of a gas or non-polar liquid phase.

Let us discuss the general principles of continuous gas extraction with simultaneous passage of aqueous and gas phases through the chromatomembrane cell. A substance extracted from the aqueous phase forms some zone within the mass-exchange layer (see Fig. 3) that moves bi-directionally with flows of both phases. The volume rate of shift of that zone front along the direction of aqueous phase flow W_{ZL} is expressed by the ratio known from the theory of chromatography:

$$W_{ZL} = \frac{W_L}{1 + (V_G/V_L)K} \quad (8)$$

where W_L is the linear rate of the aqueous phase

movement with respect to the mass-exchange layer, V_G/V_L the volume ratio of gas to liquid phase within the cell and K the coefficient of the component distribution in a gas-liquid system [the ratio of the component equilibrium concentrations (mol/dm^3) in the gas and liquid phases]. At the same time, the front of the substance zone will also move along the direction of gas-phase flow with a volume rate W_{ZG} :

$$W_{ZG} = \frac{W_G}{1 + (V_L/V_G)(1/K)} \quad (9)$$

When the stationary state is established, the front will occupy an invariant position at some angle to the direction of movement of each phase. The line AB in Fig. 3 reflects the stationary position of the zone front for the ideal case of no front dispersion. It is a vector sum of the rates of the component transfer with flows of both phases, the vectors being plotted from point A.

Let us consider the time t_{ZL} , the time necessary for the front to reach the outlet collector for the liquid phase, and t_{ZG} , the time to shift the front along the gas-phase direction by a distance equal to the height of the cell h (see Fig. 3a). The mode of ultimate equilibrium saturation will be realized with the condition $t_{ZL} < t_{ZG}$, assuming the absence of dispersion. According to the distribution law we have

$$C_G = C_W K \quad (10)$$

where C_G is the component concentration in an

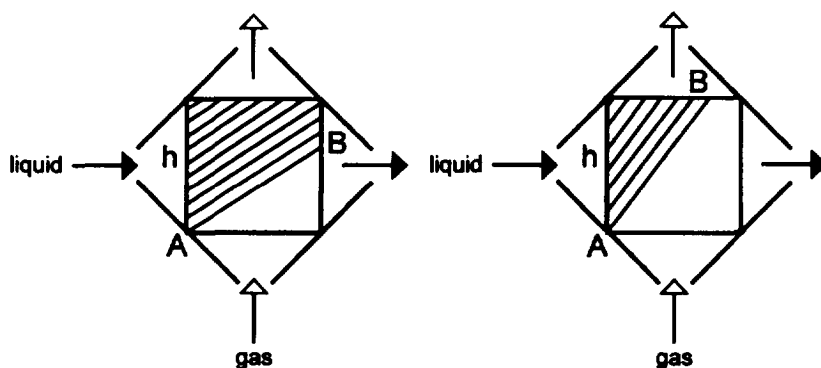


Fig. 3. Schemes of substance zone shift within a chromatomembrane cell for the modes of (left) ultimate equilibrium saturation and (right) total isolation.

extracting gas at the outlet of the chromatomembrane cell and C_w the component concentration in the initial aqueous solution. Correspondingly, with the condition $t_{zL} > t_{zG}$, we can speak of the total isolation mode, where the component concentration in liquid phase at the outlet of the chromatomembrane cell is zero (see Fig. 3b). According to the material balance equation, the following proportion will be valid:

$$C_G = C_w(W_L/W_G) \quad (11)$$

where W_G and W_L are the volume flow-rates of gas and liquid phases through the cell, respectively.

When proceeding from the obvious ratios

$$t_{zL} = V_L/W_{zL} \quad (12)$$

and

$$t_{zG} = V_G/W_{zG}, \quad (13)$$

while inserting Eqs. 8 and 9 into Eqs. 12 and 13, respectively, we obtain

$$t_{zL} = (V_L + V_G K)/W_L \quad (14)$$

$$t_{zG} = (V_L + V_G K)/KW_G \quad (15)$$

Consequently, the condition of the mode of ultimate equilibrium saturation $t_{zL} < t_{zG}$ and that of the mode of total isolation $t_{zL} > t_{zG}$ can be written as

$$W_L/W_G > K \quad (16)$$

and

$$W_L/W_G < K \quad (17)$$

3. Experimental

A schematic diagram of the continuous chromatomembrane HSA is presented in Fig. 4. An aqueous sample with a known content of analyte component is passed at a certain flow-rate through the regulatory valve and the inlet collector into the mass-exchange layer of the chromatomembrane cell and then to waste through the outlet collector. Simultaneously, the extracting gas (nitrogen or helium) is passed by the common chromatographic feed regulator and

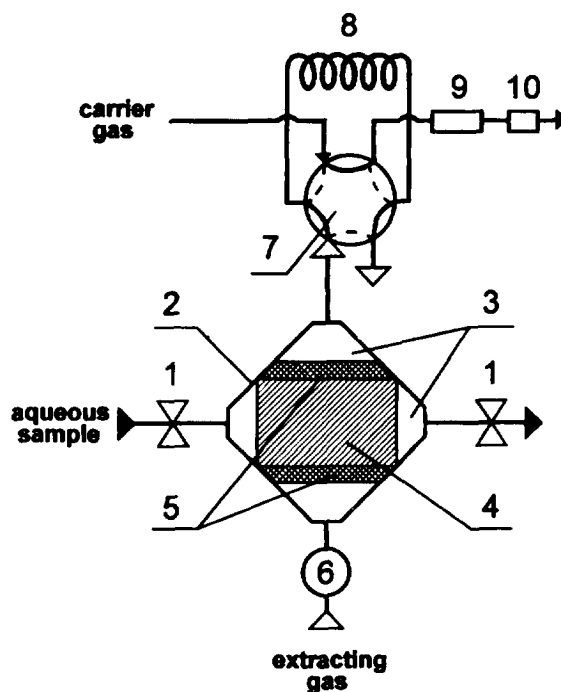


Fig. 4. Schematic diagram of chromatomembrane headspace analysis. 1 = Regulating valve; 2 = case of the chromatomembrane cell; 3 = collector; 4 = mass-exchange layer of the cell; 5 = microporous membrane; 6 = feed regulator; 7 = sampling valve of gas chromatograph; 8 = sampling loop; 9 = chromatographic column; 10 = detector.

the inlet collector at a certain flow-rate through the microporous membranes and mass-exchange layer, then from the outlet collector to the loop of the sampling valve of the gas chromatograph. The valve periodically injects the gas sample into the chromatograph to determine content of analyte components in the extracting gas. The coefficient of extraction of the components from aqueous solution into the gas flow was determined for a stationary working regime of the chromatomembrane cell. For this purpose the solution from the inlet of the cell was analysed by means of gas chromatography with liquid-gas preconcentration [9].

Model aqueous solutions of analyte components were prepared by dissolution of known amounts of analytical-reagent grade compounds in distilled water. A Tsvet-560 laboratory gas chromatograph was used for determination of

substances extracted from aqueous solution. Two configurations were used for the determination of organic compounds and inorganic gases. In the former case the chromatograph was equipped with 2-m columns packed with Polysorb-1 and a flame ionization detector and in the latter with 2-m columns packed with zeolites CaA and a thermal conductivity detector. In the latter configuration the extracting gas was passed through a drying tube packed with silica gel before entering the loop of the sampling valve.

The chromatomembrane cells under investigation had a mass-exchange layer made of biporous PTFE. The manufacturing details are presented elsewhere [10]. The mass-exchange layer is analogous in its structure to the sorbent packing in liquid–liquid and liquid–gas chromatographic columns [9], the macropores being equivalent to the space between sorbent granules in the column. Our technology provides the successive formation of microporous structure with a mean pore radius of ca. $0.5 \mu\text{m}$ and a biporous structure with a mean radius of macropores of ca. 0.5 mm . The upper limit of $2 \mu\text{m}$ was found for the micropore size from the pressure that corresponds to water breakthrough. The dimensions of the mass-exchange layer are presented hereafter in the form length \times width \times height. The length is measured along the aqueous phase flow and the height along the gas passage direction. The thickness of the microporous membranes is 0.75 mm . The cells in this study allow the aqueous phase flow-rate to be varied within the range $0\text{--}300 \text{ cm}^3/\text{min}$ and the extracting gas flow-rate within the range $0\text{--}500 \text{ cm}^3/\text{min}$.

4. Results and discussion

As follows from theoretical consideration of the chromatomembrane process (see above), there are two boundary modes for continuous chromatomembrane HSA: ultimate equilibrium saturation and total isolation. Fig. 5 presents experimental data for the volatile component concentration in extracting gas as a function of the ratio of volume flow-rates for aqueous and gas phases (curve 1). One can subdivide this plot

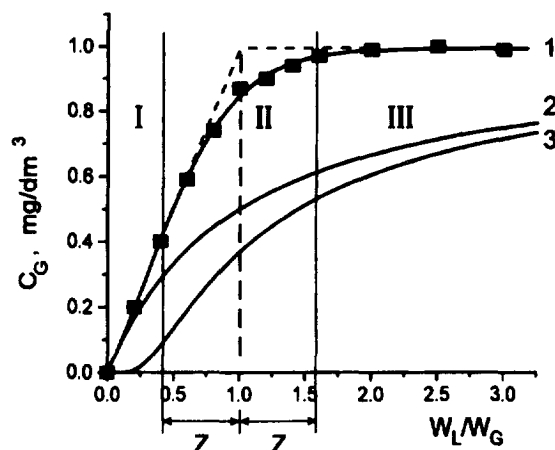


Fig. 5. Acetylene ($K = 0.99$) content in the extracting gas (C_G) as a function of the flow-rate ratio of an aqueous sample to the extracting gas (W_L/W_G). Acetylene content in the sample, $1 \text{ mg}/\text{dm}^3$. (1) Continuous chromatomembrane extraction. Aqueous sample flow-rate, $20 \text{ cm}^3/\text{min}$. Chromatomembrane cell dimensions $2 \times 0.8 \times 1 \text{ cm}$. I = Area of virtually total isolation; II = intermediate area; III = area of ultimate equilibrium saturation. (2) Countercurrent gas extraction (stripping or membrane permeation). Calculation according to Eq. 20. (3) Common dynamic gas extraction with stationary liquid (calculation according to Eq. 21).

into three parts. The first corresponds to the total isolation mode where Eq. 11 is sufficiently valid. The second part is an intermediate area of partial isolation (or partial saturation). The third part corresponds to the mode of ultimate equilibrium saturation where Eq. 10 is valid when substituting the value of distribution coefficient ($K = 0.99$ for acetylene). The first and the third parts of the plot are linear and they are extrapolated with dashed lines to the intersection point. The abscissa of this point corresponds with high accuracy to the theoretical boundary between areas of ultimate saturation and total isolation (Eqs. 16 and 17), i.e., to the value of the distribution coefficient of acetylene.

The existence of the intermediate area is caused by dispersion of the zone front in the chromatomembrane cell, which we did not take into account within the framework of the theoretical discussion. Considering this zone dispersion, one can rewrite the boundary conditions for

the modes of ultimate equilibrium saturation and total isolation more rigorously as

$$W_L/W_G > K + Z \quad (18)$$

and

$$W_L/W_G < K - Z \quad (19)$$

where Z is a characteristic of the given chromatomembrane cell that accounts for the dispersion of the substance front within it. The Z value for experimental cells was about 30–60% of the K within studied range of flow-rates.

Fig. 5 allows one also to compare the results obtained by the chromatomembrane method with traditional methods of analysis. It presents calculated plots for the variation of acetylene concentration vs. variation in W_L/W_G ratio for different HSA versions. Curve 2 corresponds to countercurrent gas extraction performed as bubbling after the stationary state has been established. It is calculated according to [11]

$$C_G = \frac{C}{1/K + W_G/W_L} \quad (20)$$

Eq. 20 is also valid as well for the case of extraction of substances into the gas phase through a permeable membrane [12]. Curve 3 corresponds to the common dynamic gas extraction. It is calculated according to the known equation [13]

$$C_G = KC \exp(-V_G K/V_L) \quad (21)$$

Here the ratio of liquid and gas phase volumes, V_L/V_G , is plotted on the x -axis instead of the ratio of fluxes, W_L/W_G . It is obvious from Fig. 4 that, in the chromatomembrane HSA, the acetylene concentration in the extracting gas is substantially higher over all the range of W_L/W_G ratio than in any common HSA version.

The mode of ultimate equilibrium saturation can be realized in all HSA versions. However, for common HSA versions, Eq. 10 will be valid with an accuracy better than 1% only with $W_L/W_G > 100K$, according to Eqs. 20 and 21. At the same time, a W_L/W_G about twice as high as K is sufficient for the chromatomembrane version. The mode of virtually total isolation is realized only with very low W_L/W_G ratios in the common

HSA versions. The component concentration in the extracting gas is essentially lower than can be reached in the chromatomembrane process because of the wider area where Eq. 11 is valid.

Fig. 6 presents plots for the concentration of volatile organic compounds (VOC) extracted into the gas phase for W_L/W_G ratios characteristic of the mode of ultimate equilibrium saturation. All the concentrations of components in the extracting gas correspond to the ultimate values obtained from Eq. 10 within all the W_L/W_G range that fit Eq. 18. The mode of equilibrium saturation is the most efficient one for continuous chromatomembrane HSA of polar and less volatile VOC with $K < 1$. At the same time, the ability to have a broad variation in the flow-rates of phases through the chromatomembrane cell also permits the analysis of components with $K > 1$.

If equilibrium saturation is achieved within the chromatomembrane cell, one can calculate the limits of detection of VOC in aqueous solutions by the chromatomembrane HSA from the known K data and the sensitivity of GC detectors with respect to those compounds. Table 1 presents such detection limits evaluated for the

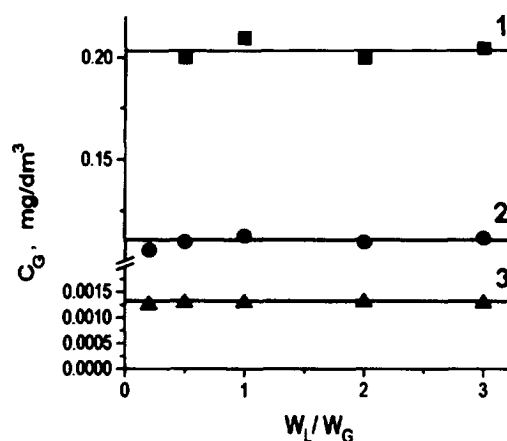


Fig. 6. VOC content in the extracting gas (C_G) as a function of the flow-rate ratio of an aqueous sample to the extracting gas (W_L/W_G). Chromatomembrane cell dimensions, $20 \times 5 \times 0.8$ cm. Aqueous sample flow-rate $50 \text{ cm}^3/\text{min}$. Content of components in the sample, $1 \text{ mg}/\text{dm}^3$. 1 = Benzene ($K = 0.2$); 2 = chloroform ($K = 0.11$); 3 = acetone ($K = 0.0013$).

Table 1

Detection limits for some VOC using chromatomembrane HSA in the equilibrium saturation mode

Compounds	$K \times 10^2$	Limit of detection in aqueous solution ($\mu\text{g}/\text{dm}^3$)
Alkanes, C_1 – C_8	600–3000	0.03–0.2
Alkenes, C_1 – C_8	300–2000	0.05–0.3
Aromatic hydrocarbons, C_6 – C_8	20–50	2–5
Chlorinated hydrocarbons, C_1 – C_3	4–100	1–25
Ethers, C_2 – C_4	2–20	5–50
Esters (acetic), C_3 – C_7	0.2–1.0	100–500
Aldehydes, C_2 – C_5	0.5–2.0	50–200
Methylketones C_3 – C_6	0.3–2.0	50–300

analysis of some VOC using a flame ionization detector. The significant result of equilibrium saturation of phases within the chromatomembrane cell also provides the possibility of using the chromatomembrane method in the production of standard gas mixtures with preset contents of organic compounds.

The mode of total isolation is preferable for the determination of non-polar inorganic gases and non-polar VOC with $K > 1$ in aqueous solutions, when low detection limits are not necessary. In this case, small temperature oscillations and other factors affecting the K value are not so significant as in the equilibrium saturation mode. The accuracy of analysis here will depend to a crucial extent on the accuracy of keeping constant the flow-rates through the cell. Fig. 7 shows experimental variations in the concentrations of oxygen, nitrogen and hexane in the extracting gas vs. the ratio of flow-rates of aqueous and gas phases for the continuous total isolation mode. The concentrations of components in the initial aqueous solutions were kept constant. It is seen that the variations correspond to Eq. 11 fairly strictly within a broad range of W_L/W_G values. The total isolation mode allows the determination of non-polar hydrocarbons in water at the level of a few tenths of $\mu\text{g}/\text{dm}^3$ with a flame ionization detector and the determination of non-polar inorganic gases such as oxygen or nitrogen at the level of few hundredths of $\mu\text{g}/\text{dm}^3$ with a thermal conductivity detector.

Both modes of chromatomembrane HSA pro-

vide a high reproducibility of results. The relative mean-square deviation is less than 0.02–0.05. The choice of optimum flow-rates depends on the mode of the process and originates from a compromise between the requirements for the detection limits and the response time of the detection system. It takes from several seconds to a few minutes for the stationary state of the chromatomembrane process to settle. This time depends on the mode chosen, the distribution

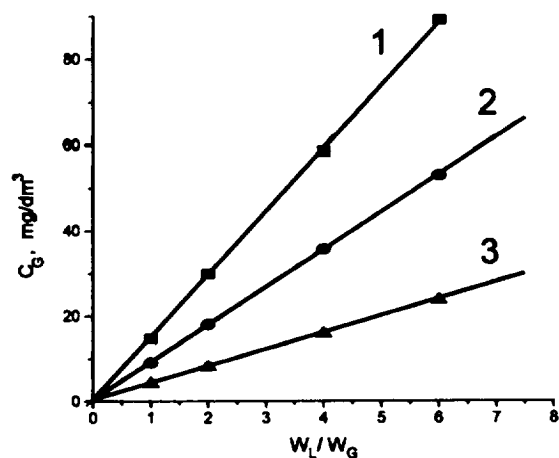


Fig. 7. Content of components in the extracting gas (C_G) as a function of the flow-rate ratio of an aqueous sample to the extracting gas (W_L/W_G). Chromatomembrane cell dimensions, $5 \times 4 \times 0.8$ cm. Aqueous sample flow-rate, $20 \text{ cm}^3/\text{min}$. Concentrations of components in the sample: nitrogen, 15; oxygen, 9; hexane, $4 \text{ mg}/\text{dm}^3$. 1 = Nitrogen ($K = 63$); 2 = oxygen ($K = 31$); 3 = hexane ($K = 20$).

coefficients, the ratio of flow-rates and parameters of the mass-exchange layer.

5. Conclusion

The boundary conditions for the realization of the chromatomembrane process in a liquid–gas system have been determined. The principles for front formation of zones of extracted substances in the chromatomembrane cell have been discussed. The appropriate mode of chromatomembrane gas extraction in headspace analysis can be chosen on the basis of the above considerations. The advantages of the new HSA version were shown in comparison with the traditional schemes. The limits of VOC detection by means of the chromatomembrane HSA were calculated for the mode of equilibrium saturation.

Acknowledgements

This investigation was supported by ISF grant R 49000 and by grant 08138 from the Russian Foundation on Fundamental Researches.

References

- [1] H. Hachenberg and A.P. Schmidt, *Gas Chromatographic Head-Space Analysis*, Heyden, London, 1977.
- [2] B.V. Ioffe and A.G. Vitenberg, *Head-Space Analysis and Related Methods in Gas Chromatography*, Wiley, New York, 1984.
- [3] A.G. Vitenberg, *J. Chromatogr.*, 556 (1991) 1.
- [4] A.P. Bianchi, M.S. Varney and J. Phillips, *J. Chromatogr.*, 557 (1991) 429.
- [5] L. Lepine and J.-F. Archambault, *Anal. Chem.*, 64 (1992) 810.
- [6] G. Baykut, *Rev. Sci. Instrum.*, 63 (1992) 3196.
- [7] J.G. Schnable, M.B. Capangpangan and I.H. (Mel)Suffet, *J. Chromatogr.*, 549 (1991) 335.
- [8] L.N. Moskvina, *J. Chromatogr. A*, 669 (1994) 81.
- [9] L.N. Moskvina and O.V. Rodinkov, *CRC Crit. Rev. Anal. Chem.*, 24 (1994) 317.
- [10] L.N. Moskvina et al., *Russ. Pat.*, 2 023 488.
- [11] A.N. Marinichev, A.G. Vitenberg and A.S. Bureiko, *J. Chromatogr.*, 600 (1992) 251.
- [12] E. Kozłowski, E. Sienkowska-Zyskowska and T. Gorecki, *Fresenius' Z. Anal. Chem.*, 320 (1985) 341.
- [13] A.G. Vitenberg and B.V. Ioffe, *J. Chromatogr.*, 471 (1989) 55.